DOI 10.1007/s10946-024-10211-8
Journal of Russian Laser Research, Volume 45, Number 3, May, 2024

LIGHT–MATTER ENTANGLEMENT IN A MICROCAVITY WITH A QUANTUM WELL AND INJECTED WITH SQUEEZED LIGHT

Desalegn Ayehu[1] and Lmenew Alemu[2]

[1]*Department of Physics, Addis Ababa University*
Addis Ababa, Ethiopia

[2]*Department of Physics, Wollo University*
Dessie, Ethiopia

*Corresponding author e-mail: desalegnayehu2@gmail.com

Abstract

We investigate the quantification of entanglement between the photonic and excitonic modes in a semiconductor microcavity injected with squeezed light. By deriving and subsequently establishing the solutions to the quantum Langevin equations, we quantify the transient entanglement and the steady-state entanglement between the photonic and excitonic modes in the low-excitation regime. It turns out that the cavity mode and the exciton mode are entangled in both the weak and strong coupling regimes, and there is the entanglement between the cavity mode and the exciton mode even in the absence of direct coupling between them. Furthermore, though the transit entanglement increases with the squeeze parameter, it decreases with the initial average intensity of the cavity mode. Also, we demonstrate that, in the strong coupling regime, the steady-state entanglement grows with coupling strength while, in the weak coupling regime, it decreases.

Keywords: entanglement, quantum well, exciton, polariton.

1. Introduction

Extensive researches have been carried out to quantify the photon–photon entanglement in the past few years [1–5]. This is because the entanglement between two field modes has been widely utilized in basic tests of quantum physics [6] and in quantum information processing [7]. Several models have been developed for the generation of photon–photon entanglement in the last few years; one of the most common schemes is the correlated emission laser [8–10]. For instance, the entanglement between the field modes due to a correlated emission laser and the coherence induced through the coherent superposition of the top and ground levels of the injected atoms has been investigated in [3], taking into consideration the environment-induced decoherence. Subsequently, such schemes as three-level and four-level quantum beat lasers were introduced because of the coherence provided by the external coherent field [11, 12]. Entanglement occurs not only between the field modes; the matter modes can also be the source of entangled states [13–15], which are employed to store and locally manipulate quantum information in continuous-variable quantum networks. In addition, these systems are not susceptible to the environmental degrees of freedom that cause the phenomenon of decoherence.

Recently, different candidates have been introduced for manipulating and storing quantum information. Semiconductor cavity quantum electrodynamics (QED) is one of the most interesting fields of

Manuscript submitted by the authors in English on May 16, 2024.

 1071-2836/24/4503-0268

research, with both practical applications and fundamental implications [16–19]. In regard to the basic features, semiconductor cavity QED provides a platform for studying the interaction between the exciton and confined photon in optical cavities, and, in the realm of practical application, semiconductor cavity QED offers the potential to create optical devices with unique properties for quantum computing [20, 21]. In a semiconductor microcavity, the Coulomb interaction between the hole in the valence band and the excited electron in the conduction band creates an exciton. This interaction is strongly coupled with the electromagnetic field in the cavity, forming the cavity polariton.

The squeezing properties of the excitonic mode in a microcavity with a quantum well and injected with squeezed light were presented in [22, 23]. The squeezing of the excitonic mode grows with increase in the squeeze parameter. The nonclassical features of the fluorescent light generated by a quantum well in a microcavity with a nonlinear medium were considered in [24, 25]. The authors showed that the fluorescent light demonstrated squeezing and bunching, with the degree of squeezing depending on the amplitude of the pump mode. In addition, the entanglement between the photon and exciton in a semiconductor microcavity containing a quantum well was considered in [26], applying the Wehrl entropy and the generalized concurrence. The authors showed that strong coupling between the environment and the system decreased the amount of entanglement.

In this study, we explore the photon–exciton entanglement in a semiconductor microcavity with a quantum well and the input squeezed light. The considered scheme has attractive applications in quantum information science, such as quantum teleportation, entanglement swapping, and linear quantum computation. Our study is limited to the weak excitation regime, where the amount of excitons in the microcavity is very low to ignore the exciton–exciton interaction. Recently, the squeezing and statistical features of the exciton mode in a semiconductor microcavity driven by external coherent light and injected with squeezed light have been investigated in [27], where the authors showed that the exciton-mode squeezing relied on the exciton–photon detuning. Moreover, the intensity and squeezing spectra of a hybrid optomechanical system with an optical cavity containing a quantum well were studied in [28] by applying the solutions to the quantum Langevin equations; the authors showed that the input squeezed light influenced the intensity spectrum in the hybrid resonance regime.

Unlike the previous studies, where the emphasis was on statistical and squeezing properties, in our study here, we devote ourselves to investigating the photon–exciton entanglement in a microcavity with a quantum well coupled to a broadband squeezed vacuum. We demonstrate to what extent the transient entanglement and steady-state entanglement of the photon–exciton modes depend on the system variables, using the the Duan–Giedke–Cirac–Zoller (DGCZ) criterion [29] and the logarithmic negativity (LG) [30–32]. We apply the solutions to the quantum Langevin equations for the field and exciton modes to study the steady-state entanglement as well as transient entanglement between the cavity mode and excitonic mode.

2. Model and Master Equation

We consider a microcavity made of two Brag reflecting mirrors with a quantum well coupled to a single-mode squeezed vacuum reservoir; see Fig. 1. In order to excite an electron in the conduction band, the input squeezed light interacts with the quantum well. This results in a hole in the valence band and the creation of an exciton, when the hole in the valence

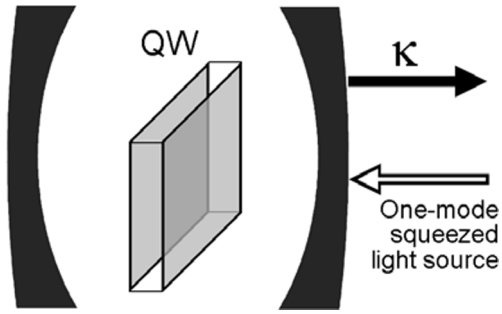

Fig. 1. Scheme of a semiconductor microcavity containing a quantum well and coupled to broadband squeezed light.

band interacts with the electron in the conduction band.

The Hamiltonian of the system under study is given by

$$\hat{H}_I = \Delta' \hat{a}_2^\dagger \hat{a}_2 + ig(\hat{a}_1^\dagger \hat{a}_2 - \hat{a}_1 \hat{a}_2^\dagger), \tag{1}$$

where $\hat{a}_1$ ($\hat{a}_1^\dagger$) and $\hat{a}_2$ ($\hat{a}_2^\dagger$) are the annihilation (creation) operators for the field mode and the exciton mode, respectively, g is coupling strength between the field mode and the exciton mode, and $\Delta' = \omega_e - \omega_p$; also, ω_e (ω_p) represents the exciton (photon) frequency.

The master equation for the scheme under investigation, with the damping of the microwave mode by broadband squeezed light and the excitonic mode by a vacuum reservoir, has the form

$$\begin{aligned}\frac{d\hat{\rho}}{dt} &= -i[\Delta' \hat{a}_2^\dagger \hat{a}_2, \hat{\rho}] + g[\hat{a}_1^\dagger \hat{a}_2 - \hat{a}_1 \hat{a}_2^\dagger, \hat{\rho}] + \frac{1}{2}\varkappa[N+1](2\hat{a}_1 \hat{\rho} \hat{a}_1^\dagger - \hat{a}_1^\dagger \hat{a}_1 \hat{\rho} - \hat{\rho} \hat{a}_1^\dagger \hat{a}_1) \\ &+ \frac{1}{2}\varkappa N(2\hat{a}_1^\dagger \hat{\rho} \hat{a}_1 - \hat{a}_1 \hat{a}_1^\dagger \hat{\rho} - \hat{\rho} \hat{a}_1 \hat{a}_1^\dagger) + \frac{\varkappa}{2} M(2\hat{a}_1 \hat{\rho} \hat{a}_1 - \hat{a}_1^2 \hat{\rho} - \hat{\rho} \hat{a}_1^2 + 2\hat{a}_1^\dagger \hat{\rho} \hat{a}_1^\dagger - \hat{a}_1^{\dagger 2} \hat{\rho} - \hat{\rho} \hat{a}_1^{\dagger 2}) \\ &+ \frac{\gamma}{2}(2\hat{a}_2 \hat{\rho} \hat{a}_2^\dagger - \hat{a}_2^\dagger \hat{a}_2 \hat{\rho} - \hat{\rho} \hat{a}_2^\dagger \hat{a}_2),\end{aligned} \tag{2}$$

where $\varkappa$ is decay rate of the field mode, γ is the dissipation rate of the exciton by the spontaneous emission, $N = \sinh^2(r)$, and $M = \cosh(r)\sinh(r)$, with r being the parameter defining the squeezed light.

Taking into account the master equation, we determine the Langevin equations; they read

$$\frac{d}{dt}\hat{a}_1 = -\frac{\varkappa}{2}\hat{a}_1 + g\hat{a}_2 + \hat{f}_1(t), \tag{3}$$

$$\frac{d}{dt}\hat{a}_2 = -\left(i\Delta' + \frac{\gamma}{2}\right)\hat{a}_2 - g\hat{a}_1 + \hat{f}_2(t), \tag{4}$$

where $\hat{f}_1(t)$ is the reservoir noise operator for the cavity mode, which has the following non-vanishing correlation functions:

$$\langle \hat{f}_1(t)\hat{f}_1(t')\rangle = \langle \hat{f}_1^\dagger(t)\hat{f}_1^\dagger(t')\rangle = \varkappa M\delta(t-t'), \tag{5}$$

$$\langle \hat{f}_1(t)\hat{f}_1^\dagger(t')\rangle = \varkappa(N+1)\delta(t-t'), \qquad \langle \hat{f}_1^\dagger(t)\hat{f}_1(t')\rangle = \varkappa N\delta(t-t'). \tag{6}$$

The operator $\hat{f}_2(t)$ denotes the noise operator characterizing the coupling of the exciton mode with the vacuum reservoir; it has the following non-vanishing correlation function:

$$\langle \hat{f}_2(t)\hat{f}_2^\dagger(t')\rangle = \gamma\delta(t-t'). \tag{7}$$

In this work, we are interested in the situation, where the cavity decay rate is equal to the exciton dissipation rate through the spontaneous emission, and the cavity mode frequency coincides with the exciton mode frequency. Thus, in view of these considerations and the assumption that $\varkappa = \gamma = \Gamma$, we can combine Eqs. (3) and (4) and arrive at

$$\frac{d}{dt}\hat{x}_\pm = -\lambda_\pm \hat{x}_\pm + \hat{f}_\pm(t), \tag{8}$$

where

$$\hat{x}_\pm = \hat{a}_1 \pm i\hat{a}_2, \qquad \lambda_\pm = \frac{\Gamma}{2} \pm ig, \qquad \hat{f}_\pm(t) = \hat{f}_1(t) \pm i\hat{f}_2(t). \tag{9}$$

Thus, the formal solution to Eq. (8) reads

$$\hat{x}_{\pm}(t) = \hat{x}_{\pm}(0)e^{-\lambda_{\pm}t} + \int_0^t e^{-\lambda_{\pm}(t-t')}\hat{f}_{\pm}(t')\ dt'. \tag{10}$$

Now applying Eqs. (9) and (10), we can establish the following relations:

$$\hat{a}_1(t) = F(t)\hat{a}_1(0) + G(t)\hat{a}_2(0) + \int_0^t F(t-t')\hat{f}_1(t')\ dt' + \int_0^t G(t-t')\hat{f}_2(t')\ dt', \tag{11}$$

$$\hat{a}_2(t) = -G(t)\hat{a}_1(0) + F(t)\hat{a}_2(0) - \int_0^t G(t-t')\hat{f}_1(t')\ dt' + \int_0^t F(t-t')\hat{f}_2(t')\ dt', \tag{12}$$

where

$$F(t) = \cos(gt)e^{-\Gamma t/2} \qquad \text{and} \qquad G(t) = \sin(gt)e^{-\Gamma t/2}. \tag{13}$$

3. Solutions of the Cavity Mode Operator and the Exciton Mode Operator

Here, we seek to determine the average values of different products of the field mode operators and the exciton mode operators by applying the fundamental equations, which appear in Eqs. (11) and (12). To this end, making use of these equations and based on the assumption that the field and the exciton modes are initially in Fock states, along with the information that the field mode operator and the exciton mode operator are not correlated with their corresponding Langevin noise forces at the initial time, we can write that

$$\begin{aligned}
&\langle \hat{a}_1(t)\hat{a}_2(t)\rangle = \\
&-\int_0^t\int_0^t F(t-t')G(t-t'')\langle \hat{f}_1(t')\hat{f}_2(t'')\rangle\, dt'\, dt'' + \int_0^t\int_0^t F(t-t')F(t-t'')\langle \hat{f}_1(t')\hat{f}_2(t'')\rangle\, dt'\, dt'' \\
&-\int_0^t\int_0^t G(t-t')G(t-t'')\langle \hat{f}_2(t')\hat{f}_1(t'')\rangle\, dt'\, dt'' + \int_0^t\int_0^t G(t-t')F(t-t'')\langle \hat{f}_2(t')\hat{f}_2(t'')\rangle\, dt'\, dt''.
\end{aligned} \tag{14}$$

Then, using the correlation functions for the cavity and exciton Langevin noise operators and carrying out the integration, we readily arrive at

$$\langle \hat{a}_1(t)\hat{a}_2(t)\rangle = \frac{-\Gamma M}{2(\Gamma^2+4g^2)}\left(2g - 2g\cos(2gt)e^{-\Gamma t} - \Gamma\sin(2gt)e^{-\Gamma t}\right). \tag{15}$$

One can calculate the following relations by applying the same techniques:

$$\begin{aligned}
\langle \hat{a}_2^{\dagger}(t)\hat{a}_2(t)\rangle &= \sin^2(gt)e^{-\Gamma t}n_c + \cos^2(gt)e^{-\Gamma t}n_e + \frac{N}{2(\Gamma^2+4g)} \\
&\quad\times\left(4g^2(1-e^{-\Gamma t}) - \Gamma^2 e^{-\Gamma t} + \Gamma^2\cos(2gt)e^{-\Gamma t} - 2g\Gamma\sin(2gt)e^{-\Gamma t}\right),
\end{aligned} \tag{16}$$

$$\langle \hat{a}_2^2(t)\rangle = \frac{M}{2(4g^2+\Gamma^2)}\left(4g^2(1-e^{-\Gamma t}) - \Gamma^2 e^{-\Gamma t} + \Gamma^2\cos(2gt)e^{-\Gamma t} - 2g\Gamma\sin(2gt)e^{-\Gamma t}\right), \tag{17}$$

$$\langle \hat{a}_1\hat{a}_2^\dagger\rangle = -\cos(gt)\sin(gt)e^{-\Gamma t}(n_c+1) + \sin(gt)\cos(gt)e^{-\Gamma t}(n_e+1) - \frac{\Gamma N}{2(\Gamma^2+4g^2)} \times\left(2g - 2g\cos(2gt)e^{-\Gamma t} - \Gamma\sin(2gt)e^{-\Gamma t}\right), \tag{18}$$

$$\langle \hat{a}_1^\dagger\hat{a}_2\rangle = -\cos(gt)\sin(gt)e^{-\Gamma t}n_c + \sin(gt)\cos(gt)e^{-\Gamma t}n_e - \frac{\Gamma N}{2(\Gamma^2+4g^2)} \times\left(2g - 2g\cos(2gt)e^{-\Gamma t} - \Gamma\sin(2gt)e^{-\Gamma t}\right), \tag{19}$$

$$\langle \hat{a}_1^\dagger(t)\hat{a}_1(t)\rangle = \sin^2(gt)e^{-\Gamma t}n_e + \cos^2(gt)e^{-\Gamma t}n_c + \frac{N}{2(\Gamma^2+4g^2)} \times\left(4g^2(1-e^{-\Gamma t}) + \Gamma^2(2-e^{-\Gamma t}) - \Gamma^2\cos(2gt)e^{-\Gamma t} + 2g\Gamma\sin(2gt)e^{-\Gamma t}\right), \tag{20}$$

$$\langle \hat{a}_1^2(t)\rangle = \frac{M}{2(4g^2+\Gamma^2)}\left(4g^2(1-e^{-\Gamma t}) + \Gamma^2(2-e^{-\Gamma t}) - \Gamma^2\cos(2gt)e^{-\Gamma t} + 2g\Gamma\sin(2gt)e^{-\Gamma t}\right), \tag{21}$$

where n_c and n_e are the initial average intensity of the field mode and the exciton mode.

4. Entanglement between the Cavity Mode and the Exciton Mode

In this section, we investigate the field–exciton entanglement in a microcavity containing a quantum well. Entanglement is a unique feature of a composite system, where a measurement done in one subsystem of the composite system influences the quantum state of the other subsystem. The detection of entanglement between the field modes emitted by correlated emission laser [3, 5, 33] and quantum beat laser [12, 16] have been intensively investigated by several authors. They showed the existence of the entanglement between the cavity modes in a correlated emission laser, and the bipartite entanglement depended on the rate of atomic injection. To quantify the bipartite entanglement between the photon and the exciton, we employ the Duan–Giedke–Cirac–Zoller (DGCZ) criterion and the logarithmic negativity.

4.1. DGCZ Criterion

Here, we consider the DGCZ entanglement criterion to quantify the field–exciton entanglement in a semiconductor microcavity. Within the DGCZ criterion, the condition for the field mode and the exciton mode to be entangled takes place if the variances of any two operators $\hat{s}$ and $\hat{t}$ of the field mode and the exciton mode obey the following relation:

$$(\Delta\hat{s})^2 + (\Delta\hat{t})^2 < 2, \tag{22}$$

with

$$\hat{s} = \frac{\hat{x}_a + \hat{x}_b}{\sqrt{2}}, \qquad \hat{t} = \frac{\hat{p}_a - \hat{p}_b}{\sqrt{2}}, \tag{23}$$

while the operators

$$\hat{x}_k = \hat{k} + \hat{k}^\dagger, \qquad \hat{p}_k = \frac{\hat{k} - \hat{k}^\dagger}{i}; \qquad k = a_1, a_2 \tag{24}$$

are the quadrature fluctuating operators for the field mode and the exciton mode. In view of Eqs. (23) and (24), we obtain

$$(\Delta\hat{s})^2 + (\Delta\hat{t})^2 = 2\Big[1 + \langle\hat{a}_1^\dagger\hat{a}_1\rangle + \langle\hat{a}_2^\dagger\hat{a}_2\rangle + \langle\hat{a}_1^\dagger\hat{a_2}\rangle + \langle\hat{a}_1\hat{a}_2^\dagger\rangle \pm\frac{1}{2}(\langle\hat{a}_1^2\rangle + \langle\hat{a}_2^2\rangle + \langle\hat{a}_1^{\dagger 2}\rangle + \langle\hat{a}_2^{\dagger 2}\rangle + 2\langle\hat{a}_1\hat{a}_2\rangle + 2\langle\hat{a}_1^\dagger\hat{a}_2^\dagger\rangle)\Big]. \quad (25)$$

4.1.1. Transient Entanglement

Thus, using Eqs. (15)–(21), one can easily rewrite Eq. (25) as follows:

$$(\Delta\hat{s})^2 + (\Delta\hat{t})^2 = 2\Bigg[1 + \frac{e^{-2r}-1}{2(\Gamma^2+4g^2)}\left(8g^2(1-e^{-\Gamma t}) + 2\Gamma^2(1-e^{-\Gamma t})\right) - \frac{\Gamma(e^{-2r}-1)}{\Gamma^2+4g^2} \times \left(2g - 2g\cos(2gt)e^{-\Gamma t} - \Gamma\sin(2gt)e^{-\Gamma t}\right) + e^{-\Gamma t}(n_c+n_e) + 2\sin(gt)\cos(gt)e^{-\Gamma t}(n_e-n_c)\Bigg]. \quad (26)$$

From this expression, we see that the field–exciton entanglement is influenced by the injected squeezed light, the initial average intensity of the field mode, the photon–exciton coupling constant, and other system parameters. In the following, we present the possible cases for controlling the entanglement between the photon and the exciton by manipulating the system variables.

As one can see in Figs. 2–4, in spite of the fact that the cavity mode and exciton mode are not entangled at the initial moment, transient entanglement develops as time passes. The increased entanglement between the photon and the exciton in the microcavity could be seen as the result of their long-term interaction with one the other. In Figs. 2–4, we also show that, over time, the amplitude of oscillations diminishes and eventually reaches a flat condition at steady state.

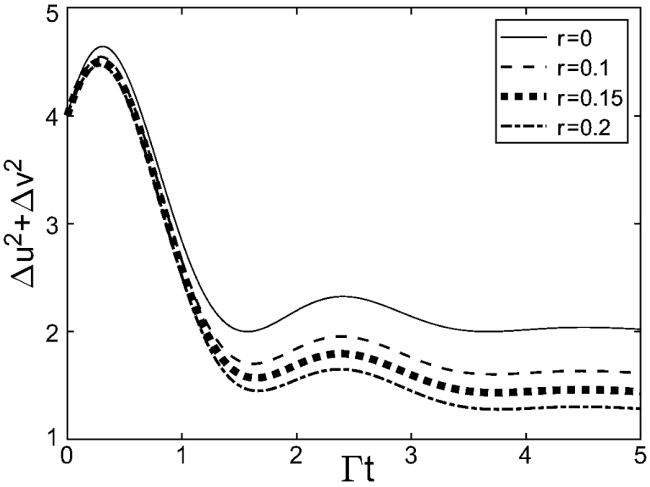

Fig. 2. Entanglement measure, Eq. (26), vs Γt for $g/\Gamma = 1.5$, $n_c = 0$, $n_e = 1$, and values of the squeeze parameter r equal to zero (the solid curve), 0.1 (the dashed curve), 0.15 (the dotted curve), and 0.2 (the dash-dotted curve).

We start by examining the dependence of the photon–exciton entanglement on the input squeezed light. In Fig. 2, we present the plots of $\Delta\hat{s}^2 + \Delta\hat{t}^2$ as a function of dimensionless time for various values of the input squeeze parameter; one can see that the photon–exciton entanglement disappears at the initial moment, irrespective of the value of the squeeze parameter r, and the entanglement increases with time. However, a considerable degree of entanglement is realized between the photon and the exciton over a longer period of time in the presence of the input squeezed light. For $r = 0$, there is no field–exciton entanglement in the entire time interval; this demonstrates that the injected squeezed vacuum is the source of quantum correlation between the field mode and the exciton mode. We also see that the transient bipartite entanglement between the photon and the exciton grows with the injected squeeze parameter, and the field mode and exciton mode are not entangled for all the time, when the field mode is coupled to a vacuum reservoir. This is because the input squeezed field, not the

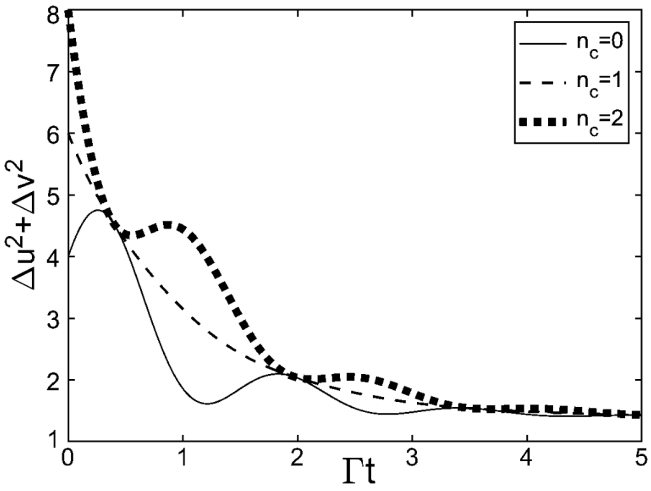

Fig. 3. Entanglement measure, Eq. (26), vs Γt for $g/\Gamma = 2$, $r = 0.1$, $n_e = 1$, and values of the initial average field photons n_c equal to 0 (the solid curve), 1 (the dashed curve), and 2 (the dotted curve).

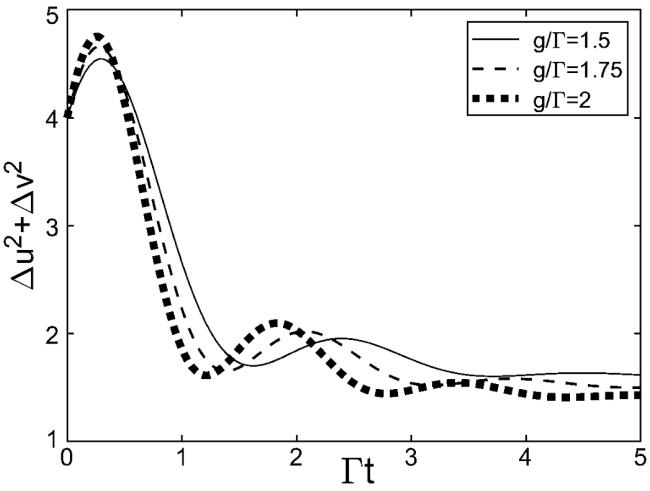

Fig. 4. Entanglement measure $\Delta s^2 + \Delta t^2$, Eq. (26), vs Γt for $r = 0.4$, $n = 0$, $\bar{n}_e = 1$, and values of g/Γ equal to 1.5 (the solid curve), 1.75 (the dashed curve), and 2 (the dotted curve).

vacuum reservoir, adds quantum coherence to the system, which leads to the creation of field–exciton entanglement.

We are also interested in studying the influence of the initial average intensity of the cavity mode on the entanglement evolution between the cavity mode and the matter mode. In Fig. 3, we present the entanglement measure as a function of dimensionless time for different values of the initial intensity of the cavity mode. The field mode and the exciton mode start to entangle first without the initial average photons, and entanglement formation between the photon and the exciton starts for $\Gamma t > 2$, when the initial average photons are present.

In Fig. 3, we also observe that the field–exciton entanglement shows oscillatory behavior for $n_c = 0$ and $n_c = 2$, but the oscillatory nature disappears for $n_c = 1$. This can be understood as the oscillatory nature of the entanglement measure vanishes for $n_c = n_e = 1$. This is because there is no transfer of energy between the field mode and the exciton mode. Also, for $n_c = 2$, the photon–exciton entanglement is above the curve $n_c = 1$, while for $n_c = 0$, it is below this curve. The effect of the initial average photons is significant at the initial moment, and the influence of the initial average photons on the entanglement decreases as time passes; this is due to the damping of these initial photons via one of the port mirrors.

In Fig. 4, we show the dynamical nature of the entanglement between the cavity mode and the exciton mode for various values of g/Γ; we see that the field–exciton entanglement depends on the field–exciton coupling constant. At the initial moment, the field–exciton entanglement grows with increase in the cavity–exciton coupling constant. With a further increase in time, the entanglement decreases with the field–exciton coupling constant for a small interval of time. In the extended time frame, the entanglement increases with the cavity–exciton coupling constant. Moreover, as the field–exciton coupling strength increases, the entanglement function shows more oscillatory behavior. This is because an increase in the photon–exciton coupling strength leads to a fast transfer of energy between the field mode and the exciton mode. This, in turn, leads to increase in the Rabi frequency. Also, we observe that this increase in the field–exciton mode interaction is the reason for the generation and loss of entanglement for large g/Γ.

4.1.2. Steady-State Entanglement

Within the extended time frame, the entanglement between the cavity mode and the exciton mode becomes constant, showing the existence of steady-state entanglement. Here, we investigate the influence of the injected squeezed light on the steady-state entanglement between the cavity mode and the exciton mode. To this end, the steady-state entanglement is found to be

$$(\Delta\hat{s})^2 + (\Delta\hat{t})^2 = 2\left[1 + \frac{(e^{-2r}-1)(4g^2+\Gamma^2)}{\Gamma^2+4g^2} - \frac{2g\Gamma(e^{-2r}-1)}{\Gamma^2+4g^2}\right]. \tag{27}$$

Here, it is essential to consider two cases: the first case is the condition, in which the cavity–exciton coupling strength is much smaller than the dissipation rates, $g \ll \Gamma$ (weak coupling regime) while, in the second case, the cavity–exciton coupling constant is much greater than the dissipation rates, $g \gg \Gamma$ (strong coupling regime). To examine the effect of the input squeezed light on the steady-state field–exciton entanglement, we present in Fig. 5 the entanglement measure $\Delta s^2 + \Delta t^2$ versus g/Γ for various values of the injected squeeze parameter. It is clear, from Fig. 5, that there is the photon–exciton entanglement in the first case; this is because the cavity is coupled to a broad-band squeezed light, and the injected squeezed light can be the cause of the photon–exciton entanglement in the weak coupling regime. Also, it is not difficult to see that, for a fixed value of the injected squeeze parameter r, the amount of entanglement rapidly decreases with increase in g/Γ in the weak coupling regime and reaches the minimum for a certain value of g/Γ, irrespective of the values of the squeeze parameter. This demonstrates that the external quantum coherence of the injected squeezed light decreases as the interaction between the photon and the exciton increases. A further increase in g/Γ results in increase in the amount of entanglement between the field mode and the exciton mode in the strong coupling regime.

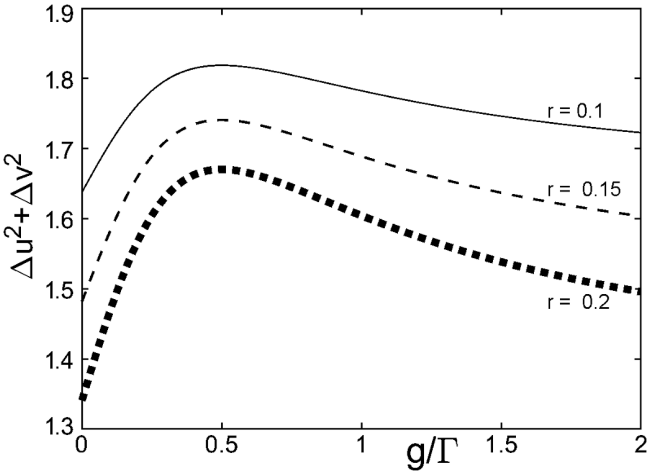

Fig. 5. Entanglement measure $\Delta s^2 + \Delta t^2$, Eq. (27), vs g/Γ for the squeeze parameter r equal to 0.1 (the solid curve), 0.18 (the dashed curve), and 0.2 (the dashed curve).

4.2. Logarithmic Negativity

We can also quantify bipartite entanglement by applying the logarithmic negativity defined by the relation

$$E_N = \max\left[0, -\log_2 V_s\right], \tag{28}$$

where $V_s = \sqrt{(\chi - \sqrt{\chi^2 - 4\det\mu})/2}$ is the smallest symplectic eigenvalue μ of the partial transposed correlation matrix of the field mode and the exciton mode, with $\chi = \det\sigma_A + \det\sigma_B - 2\det\sigma_{AB}$. Also, here, σ_A and σ_B denote the field mode and the exciton mode, while σ_{AB} denotes the correlation between the field mode and the exciton mode, and σ_A, σ_B, and σ_{AB} are related to the correlation matrix as follows:

$$\mu = \begin{bmatrix} \sigma_A & \sigma_{AB} \\ \sigma_{AB}^T & \sigma_B \end{bmatrix}. \tag{29}$$

The matrix elements of μ read

$$\mu_{mn} = \frac{1}{2}\langle \hat{X}_m \hat{X}_n + \hat{X}_n \hat{X}_m \rangle - \langle \hat{X}_m \rangle \langle \hat{X}_n \rangle, \tag{30}$$

where $m, n = 1, 2, 3, 4$ and the quadrature fluctuation operators are given by $\hat{X}_1 = \hat{a}_1 + \hat{a}_1^\dagger$, $\hat{X}_2 = \dfrac{\hat{a}_1 - \hat{a}_1^\dagger}{i}$, $\hat{X}_3 = \hat{a}_2 + \hat{a}_2^\dagger$, and $\hat{X}_4 = \dfrac{\hat{a}_2 - \hat{a}_2^\dagger}{i}$. The condition for the entanglement between the field mode and the exciton mode occurs, when $E_N > 1$. Thus, in view of Eq. (28), for E_N to be positive, $\log_2 V_s$ must be negative. This leads to the condition $V_s < 1$. Hence, the condition $V_s < 1$ is a sufficient condition for the cavity mode and the exciton mode to be entangled.

As one can see in Fig. 6, $V_s < 1$ for all values of g/Γ, and this indicates that the cavity modes and the exciton modes are entangled in both the weak and strong coupling regimes. It is also obvious in Fig. 6, that the generated entanglement decays with the coupling strength until $g/\Gamma = 0.28$ for $r = 0.4$ in the weak coupling regime. This feature of the generated entanglement between the photon and the exciton is also observed in the DGCZ criterion. Moreover, as one can see in Fig. 6, the amount of entanglement increases with increase in the squeeze parameter in the strong coupling regime. In this case, also the entanglement measure based on the DGCZ and the logarithmic-negativity criteria shows a compatible outcome. Moreover, we note that, as the input squeeze parameter increases, the maximum value of the symplectic eigenvalue shifts towards the weak coupling regime, i.e., the value of g/Γ, at which the minimum entanglement occurs, decreases. It is also revealed that the field–exciton entanglement are maximum at $g/\Gamma = 0$ (in the absence of coupling between the field mode and the exciton mode), regardless of the value of the squeeze parameter. We hope that the cause of this maximum entanglement of the photon–exciton modes is the externally injected squeezed photons. As g/Γ increases from 0 to the point, at which the minimum entanglement occurs, the input squeezed parameter has a damaging effect on the photon–exciton entanglement. With a further increase in g/Γ, the input squeeze parameter has an enhancement effect.

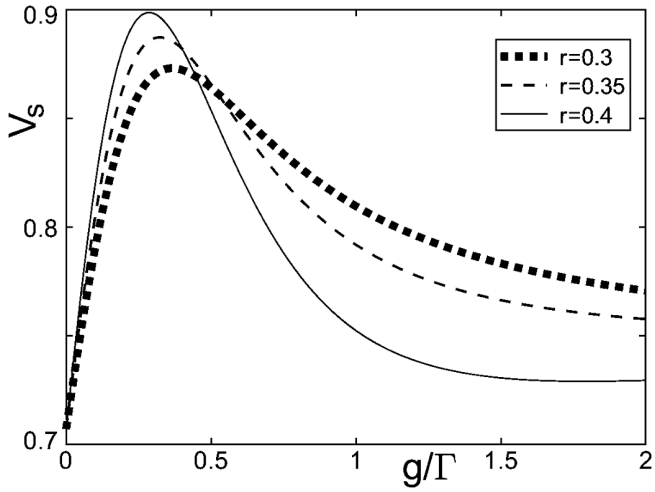

Fig. 6. The smallest eigenvalue V_s of the field–exciton modes vs g/γ for the squeeze parameter r equal to 0.3 (the solid curve), 0.35 (the dashed curve), and 0.4 (the dashed curve).

5. Conclusions

In this work, we considered a semiconductor microcavity with a quantum well and input squeezed light. The transient entanglement and steady-state entanglement between the field mode and the exciton mode were quantified, in view of the solution to the quantum Langevin equations. It turned out that the field mode and the exciton mode were not entangled at the initial moment. The entanglement between the two modes came into existence as time passed. Specifically, the transient photon–exciton

entanglement appeared first without the initial average photons. Also, we observed that the input squeezed parameter improved the transient photon–exciton entanglement whereas, in the strong coupling regime, this entanglement was hurt by the initial mean cavity photons. Moreover, there existed robust steady-state entanglement between the cavity photon and the semiconductor exciton in the absence of coupling between them. This was due to the indirect coupling that appeared between the cavity mode and the semiconductor exciton through their reservoir, despite the absence of a direct coupling between them. Like the transient entanglement, the steady-state entanglement was also enhanced by the input squeezed parameter in the strong coupling regime.

References

1. A. Fang, Y. Chen, F. Li, et al., *Phys. Rev. A*, **81**, 012323 (2010).
2. S. Qamar, F. Ghafoor, M. Hillery, and M. S. Zubairy, *Phys. Rev. A*, **77**, 062308 (2008).
3. D. Ayehu, *J. Russ. Laser Res.*, **42**, 136 (2021).
4. E. A. Sete, *Opt. Commun.*, **281**, 6124 (2008).
5. D. Ayehu, *Res. Phys.*, **28**, 104567 (2021).
6. A. Aspect, J. Dalibard, and G. Roger, *Phys. Rev. Lett.*, **49**, 1804 (1982).
7. S. L. Braunstein and H. J. Kimble, *Phys. Rev. A*, **61**, 042302 (2000).
8. D. Ayehu and A. Chane, *Ukr. J. Phys.*, **66**, 761 (2021).
9. S. Tesfa, *Phys. Rev. A*, **77**, 013815 (2008).
10. D. Ayehu and H. Ebrahim, *Int. J. Mod. Phys. B*, **38**, 2450309 (2023).
11. S. Qamar, M. Al Amri, and M. S. Zubairy, *Phys. Rev. A*, **80**, 033818 (2009).
12. R. Tahira, M. Ikram, H. Nha, and M. S. Zubairy, *Phys. Rev. A*, **83**, 054304 (2011).
13. D. Ayehu, *Res. Opt.*, **14**, 100605 (2024).
14. T. G. Tesfahannes, *J. Opt. Soc. Am. B*, **37**, 245 (2020).
15. B. Teklu, T. Byrnes, and F. S. Khan, *Phys. Rev. A*, **97**, 023829 (2018).
16. C. Weisbuch and H. Benisty, *Phys. Status Solidi B*, **424**, 2345 (2005).
17. A. Baas, J. P. Karr, H. Eleuch, and E. Giacobino, *Phys. Rev. A*, **69**, 23809 (2004).
18. P. G. Savvidis and P. G. Lagoudakis, *Semicond. Sci. Technol.*, **18**, 113 (2003).
19. E. Giacobino, J. Ph. Karr, G. Messin, and H. Eleuch, *C. R. Phys.*, **3**, 41 (2002).
20. A. Imamoglu, D. D. Awschalom, G. Burkard, et al., *Phys. Rev. Lett.*, **83**, 4204 (1999).
21. J. I. Perea and C. Tejedor, *Phys. Rev. B*, **72**, 35303 (2005).
22. D. Erenso, R. Vyas, and S. Singh, *Phys. Rev A*, **67**, 013818 (2003).
23. D. Ayehu and D. Hirpo, *Int. J. Theor. Phys.*, **62**, 125 (2023).
24. E. A. Sete, *Phys. Rev. A*, **82**, 043810 (2010).
25. E. A. Sete, H. Eleuch, and S. Das, *Phys. Rev. A*, **84**, 053817 (2011).
26. Sh. Barzanjeh and H. Eleuch, *Physica E*, **42**, 2091 (2010).
27. E. A. Sete, S. Das, and H. Eleuch, *Phys. Rev. A*, **83**, 023822 (2011).
28. H. Jabri and H. Eleuch, *Sci. Rep.*, **12**, 3658 (2022).
29. L. M. Duan, G. Giedke, J. I. Cirac, and P. Zoller, *Phys. Rev. Lett.*, **84**, 2722 (2000).
30. G. Vidal and R. F. Werner, *Phys. Rev. A*, **65**, 032314 (2002).
31. J. Laurat, G. Keller, J. O. H. Augusto, et al., *J. Opt. B*, **7**, 577 (2005).
32. G. Adesso, A. Serafini, and F. Illuminati, *Phys. Rev. A*, **70**, 022318 (2004).
33. E. A. Sete, *Opt. Commun.*, **281**, 6124 (2008).